

Review

Metal Oxide Thin Films Grafted on Silica Gel Surfaces: Recent Advances on the Analytical Application of these Materials

Yoshitaka Gushikem* and Simone S. Rosatto

Instituto de Química, UNICAMP, CP 6154, 13083-970 Campinas - SP, Brazil

Nos óxidos metálicos M_xO_y altamente dispersos como monocamadas finas sobre a superfície porosa de SiO_2 (denominados como SiO_2/M_xO_y), a ligação covalente Si-O-M formada sobre a superfície SiO_2 restringe a mobilidade dos óxidos ancorados resultando em óxidos metálicos coordenativamente insaturados (LAS) em adição aos sítios ácidos de Brønsted (BAS). Os BAS originam-se dos grupos MOH e SiOH, sendo o último devido aos grupos silanóis não reagidos. Como os óxidos ancorados estão fortemente imobilizados sobre a superfície, eles são também muito estáveis termicamente. O caráter anfotérico de muitos dos óxidos ancorados, permite a imobilização de várias espécies químicas, ácidos ou bases, resultando em uma ampla aplicação destes materiais com superfícies modificadas. Neste trabalho, muitas das recentes aplicações dos óxidos metálicos ancorados à superfície da sílica são descritas, tais como adsorventes seletivos, em processos de pré-concentração, como materiais de recheio para uso em HPLC, suporte para imobilização de enzimas, eletrodos amperométricos, sensores e biossensores.

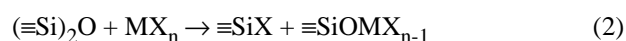
In the highly dispersed M_xO_y monolayer film on a porous SiO_2 surface, denoted as SiO_2/M_xO_y , the Si-O-M covalent bond formed on the SiO_2 surface restricts the mobility of the attached oxide resulting in coordinatively unsaturated metal oxides (LAS) in addition to the Brønsted acid sites (BAS). The BAS arise from the MOH and SiOH groups, the latter due to the unreacted silanol groups. As the attached oxides are strongly immobilized on the surface, they are also thermally very stable. The amphoteric character of most of the attached oxides allows the immobilization of various chemical species, acid or bases, resulting in a wide application of these surface modified materials. In this work many of the recent applications of these M_xO_y coated silica surfaces are described, such as selective adsorbents, in preconcentration processes, as new packing material for use in HPLC, support for immobilization of enzymes, amperometric electrodes, sensors and biosensors

Keywords: modified silica, monolayer attached metal oxides, preconcentration, modified electrodes, electrochemical sensors, biosensors

1. Introduction

The surface of silica gel contains many different types of silanol groups, $\equiv SiOH$, which can react with reagents such as metal alkoxides or halides. Preparation methods using these reagents in order to obtain active metal oxides, dispersed as monolayer films on the surface of SiO_2 , have been an area of growing interest in recent years. Experimental procedures, aiming to produce monolayers of the coating metal oxides with thermal stability, have been designed¹⁻¹³. Different from metal oxides supported on solid matrices prepared by impregnation or co-precipitation processes, grafting of the reagent on the solid surface gives rise to oxides whose acidic

properties are associated with high thermal and chemical stability, which are not characteristic of the respective oxides in the bulk phase¹⁴. From the view point of basic research, this procedure is particularly advantageous because formation of a well defined surface species allows a more precise study of the acid-base character of the active sites^{15,16}. Although SiO_2 has been considered as a relatively inert material, surface silanol groups or strained siloxane groups, as stated above, can react according to the following equations:



where MX_n is an active metal compound and $\equiv SiOH$ stands for the silanol group.

e-mail: gushikem@iqm.unicamp.br

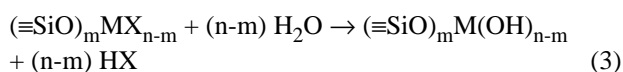
Careful hydrolysis of attached metals leads to formation of a bidimensional oxide structure in which the metals are bound to the surface by a $\equiv\text{SiO-M}$ bond. In this work some features of monolayer attached oxides on a silica gel surface are discussed.

Many of these materials have been designed to satisfy the demands of activity and selectivity in a catalytic system by a thorough control of surface morphology. For this purpose many studies have been carried out, aiming a better understanding of the surface structure of the oxide coated species^{4,6,17-22}. Thus, most of the metal oxide coated silica materials, $\text{SiO}_2/\text{M}_x\text{O}_y$, have been prepared for using in catalytic reactions^{3-5,7,10,11,23-26}.

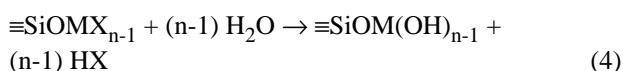
Highly dispersed metal oxides on a porous silica surface are characterized to present coordinatively unsaturated metal oxide (Lewis acid sites, LAS) in addition to the Brønsted acid sites (BAS), mainly due to the MOH groups. These LAS or BAS can adsorb many molecular species which can be immobilized by covalent bonding or electrostatic interaction. The preparation procedures, properties and applications of these species immobilized on the $\text{SiO}_2/\text{M}_x\text{O}_y$ surface, apart from applications in catalytic reactions, are described in this work. We aim to give an overview on new applications of these materials in various fields such as selective adsorbents, enzyme immobilization supports, new packing materials for HPLC columns, carbon paste modified electrodes, electrochemical sensors and biosensors.

2. Preparation and Characteristics of Oxide Monolayers

Supported active oxides are prepared as mentioned above by a careful hydrolysis of $\equiv\text{SiOMX}_{n-1}$ according to the following reaction equations:



and



It is supposed that the metal oxides form a complete and coherent layer. However in no instance, in the various examples cited in the literature, is the surface of the porous solid entirely coated. For instance, the density of niobium atoms for Nb_2O_5 coated on a SiO_2 surface²⁷, *i.e.* $\text{SiO}_2/\text{Nb}_2\text{O}_5$, is 1.7 atoms nm^{-2} while complete coverage²⁸ requires 2.2 atoms nm^{-2} . Since in most cases the porous solid specific surface areas decrease after the coating treatment, it

is not difficult to conceive that the finest pores remain untouched or blocked. In order to assure complete surface coverage, the treatment of the solid surface, *i.e.*, the reactions described by equations 1-4, can be repeated. However, treatment of the solid by successive coating of the porous surface may result in agglomeration of the particles.

3. Thermal Stability

The mobility of the oxides on the surface under thermal treatment depends on the particular metal, *i.e.* of the Si-O-M energy bond. An indication of how mobile the metal particles are on the surface is given by XPS measurements. The results are presented in Table 1.

Table 1. X-Ray photoelectron spectroscopy data for $\text{SiO}_2/\text{M}_x\text{O}_y$.

$\text{SiO}_2/\text{M}_x\text{O}_y$	Temperature /K	Atomic Ratio M/Si	Binding Energy /eV
$\text{SiO}_2/\text{Sb}_2\text{O}_5$	423	0.032	540.6 ^a
	1073	0.036	541.0
	1373	0.040	541.1
$\text{SiO}_2/\text{Nb}_2\text{O}_5$	423	0.032	210.1 ^b , 207.3 ^c
	573	0.037	210.0, 207.3
	1273	0.030	209.9, 207.2
$\text{SiO}_2/\text{TiO}_2$	473	0.088	458.7 ^d
	673	0.082	458.7
	973	0.065	458.7
	1273	0.045	458.7
$\text{SiO}_2/\text{Al}_2\text{O}_3$	423	2.51	74.7 ^e
	573	2.29	74.9
	873	2.87	75.1
	1173	2.61	75.2
	1323	1.22	75.1

^{a,b} $3d_{3/2}$, ^c $3d_{5/2}$, ^d $2p_{3/2}$, ^e $2p$

For $\text{SiO}_2/\text{Sb}_2\text{O}_5$ and $\text{SiO}_2/\text{Nb}_2\text{O}_5$, heat treatments of the samples down to 1373K, in the first case, and 1273K, in the second case, practically do not change the atomic ratio while for $\text{SiO}_2/\text{TiO}_2$, the atomic ratio decreases from 0.082 down to 0.045 between 673K and 1273K. Mobility of titanium oxide on the surface is therefore considerable if compared to that observed for antimony and niobium oxides. Diffusion of titanium into the matrix or agglomeration into larger particles may be occurring in this case. Bulk phase binding energies of the metals in the oxides are (in eV): Sb_2O_5 , $3d_{3/2} = 540.5$ ^{29,30}; Nb_2O_5 , $3d_{3/2} = 210.2$ and $3d_{5/2} = 207.4$ ³¹; TiO_2 (rutile or anatase), $2p_{3/2} = 459.0$ ³². Comparing these results with those of the metals in the coating oxides, only Sb(V), Nb(V) or Ti(IV) are detected. In every case the bulk phase oxides under heat treatment undergo phase transformations or chemical transformations at higher temperatures. For instance, the Sb $3d_{3/2}$ binding energy of Sb_2O_5 heat treated at 1373K is the same as that presented by Sb_2O_3 ³², indicating a reduction of Sb(V) to Sb(III) at this temperature. For $\text{SiO}_2/$

Nb₂O₅ heat treated at this temperature, no decomposition of Nb(V) was observed²⁷.

Bulk amorphous phase Nb₂O₅ under heat treatment becomes crystalline at *ca.* 773 K³³ while SiO₂/Nb₂O₅ at this temperature is amorphous, as shown in Figure 1(a). The X-ray diffraction patterns are the same upon heating the sample up to 1273K, Figures 1(b) and 1(c), but above this temperature, more precisely at 1573K, Figure 1(e), the material becomes crystalline, with separation of the phases and, according to the diffraction peaks, into H-Nb₂O₅ and crystalline SiO₂. An important conclusion taken from this experiment is that Nb₂O₅ is strongly attached on the silica surface and, thus, only at higher temperatures can the dispersed oxides move and agglomerate to form crystalline particles²⁷. For SiO₂/Al₂O₃, ²⁷Al NMR spectroscopy detected two species for samples heated between 423 and 1023 K, Al_{oct}(SiO₄)₆ (~ 10 ppm) and Al_{tetr}(SiO₄)₄ (~55 ppm). A third one was observed after higher heating temperature (> 1173 K) due to Al_{tbp}(SiO₄)₅ (~ 40 ppm). These observed changes of the ²⁷Al NMR spectra are due to the phase separation of Al₂O₃ on the surface³⁴.

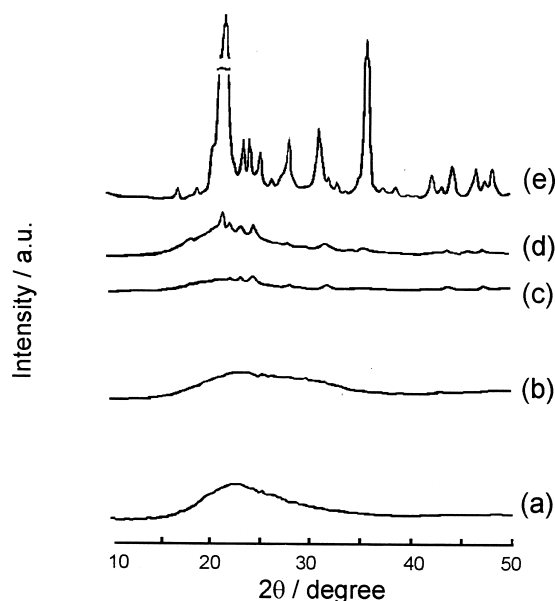


Figure 1. XRD patterns of SiO₂/Nb₂O₅ calcined at (a) 423, (b) 773, (c) 1273, (d) 1473, (e) 1573 K.

4. Acidic and Basic Properties

In most cases the attached oxides retain the acid-base properties presented by the corresponding oxides in bulk phase. However, the nature of the acid-base sites can be very different in the case of the highly dispersed oxides.

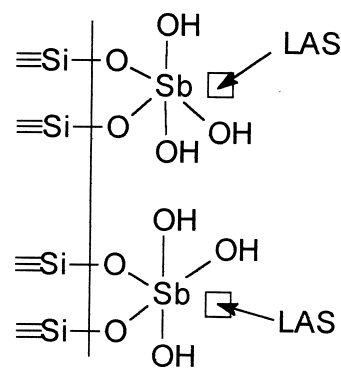
Assuming that the oxides uniformly cover the porous surface, the average metal atom density, δ , on the surface

is given by $\delta = N_f \times N / S_{\text{BET}}$, where N_f is the quantity of metal atoms (in mol g⁻¹) in the material, N is Avogadro's number and S_{BET} is the specific surface area (in nm² g⁻¹). In Table 2 the values of δ and the respective average interatomic distances, l , for some materials are presented.

Table 2. Calculated surface attached metal densities, δ , and the respective interatomic distances, l , for some materials.

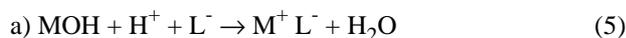
	$\delta/\text{atoms nm}^{-2}$	l/nm	Ref.
SiO ₂ /Nb ₂ O ₅	1.7	0.76	27
SiO ₂ /Sb ₂ O ₅	0.65	1.2	36
SiO ₂ /TiO ₂	2.2	0.67	12
SiO ₂ /ZrO ₂	0.65	1.2	35
SiO ₂ /SnO ₂	0.32	1.8	37

The main characteristic of these submonolayer oxides is that the atoms on the surface are separated sufficiently to allow interaction between them and, thus, they are coordinatively unsaturated. For instance, pyrochlore Sb₂O₅ (crystalline oxide) shows only Brønsted acid sites³⁸ while SiO₂/Sb₂O₅ ($\delta = 0.65$) also shows, in addition to BAS (py 19b mode at 1546 cm⁻¹), Lewis acid sites, LAS (py 8a mode at 1617 cm⁻¹ and 19b at 1456 cm⁻¹)³⁶. Such differences between the bulk structure and the highly dispersed form of antimony (V) oxide are due to the absence of a crystalline lattice in SiO₂/Sb₂O₅. Interaction of a base with LAS can occur, as shown in the Scheme 1.

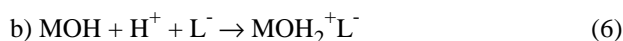


Scheme 1. Structure proposed for Sb on the surface of SiO₂. In this scheme, Sb ions are represented as coordinatively unsaturated and this is responsible for the Lewis acidity.

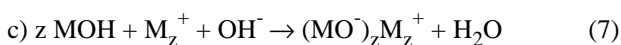
Generation of acid sites is also possible in aqueous solution on the surface of SiO₂/M_xO_y. Many of the oxides have an amphoteric character. At solution pH below the point of zero charge (pzc), they can adsorb negatively charged species according to two possible reactions³⁹⁻⁴¹:



or



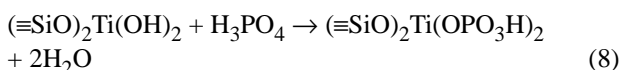
At solution pH above (pzc) they can adsorb positively charged species:



where MOH stands for the metal oxide grafted on the silica surface

As an example of anionic adsorption, as shown in equation 5 and 6, the interaction of the anionic complex $[\text{Fe}(\text{CN})_6]^{4-}$ with $\text{SiO}_2/\text{TiO}_2$ and $\text{SiO}_2/\text{ZrO}_2$ can be cited. The adherence of this species on the substrate surface is predominantly due to an ion pair interaction (equation 6). The infrared active CN stretching mode for $\text{K}_4[\text{Fe}(\text{CN})_6]$ is observed at 2041 cm^{-1} (T_{1u} mode; O_h symmetry) and, for the adsorbed species on $\text{SiO}_2/\text{TiO}_2$ or $\text{SiO}_2/\text{ZrO}_2$ surfaces, it is not shifted towards higher frequency as normally expected for M-NC bond formation⁴² nor is it split into $2A_1 + E$ (C_{4v} symmetry)^{43, 44}.

It is also possible to graft phosphate groups to the silica gel surface coated with titanium oxide:



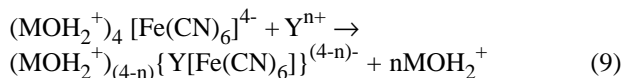
This new material was used to accumulate positively charged mediators such as Meldola's Blue or methylene blue, by ion exchange with the protons of either the phosphate groups or the hydroxyl groups on the titanium atom⁴⁵⁻⁴⁸. Experimental conditions were optimised to give the highest mediation efficiency together with the best immobilization quality.

The $[\text{Co}(\text{sepulchrate})]^{3+}$ complex immobilized on the surface of silica gel, $\text{SiO}_2/\text{ZrO}_2$ and $\text{SiO}_2/\text{ZrO}_2/\text{phosphate}$, shows electrochemical responses due to the redox process of the Co(III)/Co(II) couple⁴⁹. Acidity of the immobilized zirconium phosphate is higher than that of other matrices. Therefore, a larger amount of the cobalt complex was found and the redox potential of the Co(III)/Co(II) couple was less affected by changes in the pH values of the solutions. The electrochemical behaviour of the adsorbed complex on the matrices is affected as the pH of the solutions, as well as the nature and concentration of the supporting electrolyte, are changed.

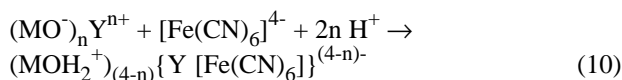
5. Reaction of the Adsorbed Species

Reactions of the adsorbed species giving rise to a new phase on the surface is also possible. For example, strongly adhered $[\text{Fe}(\text{CN})_6]^{4-}$ anion on a $\text{SiO}_2/\text{M}_x\text{O}_y$ surface, $(\text{MOH}_2^+)_4 [\text{Fe}(\text{CN})_6]^{4-}$, can react with a series of metal ions Y^{n+} forming the well known mixed valence complexes, $(\text{M}^+)_{(4-n)} \{ \text{Y}[\text{Fe}(\text{CN})_6] \}^{(4-n)-}$. The same surface species are

formed when $(\text{MO}^-)_n \text{Y}^{n+}$ reacts with $[\text{Fe}(\text{CN})_6]^{4-}$ in acid solution. The reactions that describe the formation of the complexes are:



In equation 9, the adsorbed hexacyanoferrate complex reacts with a metal ion and in the second case, equation 10,



the adsorbed metal ion reacts with the hexacyanoferrate ion at the solid-surface interface, resulting in the same mixed valence complex as in equation 9.

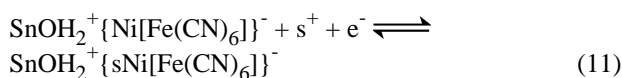
Evidence that supports formation of such structured complexes on the surface is given by the values of the midpoint potential, obtained from cyclic voltammetry measurements by using carbon paste electrodes made with these materials^{37, 43-53}. Table 3 contains the midpoint redox potentials, E_m [$E_m = (E_{pa} + E_{pc})/2$; where E_{pa} and E_{pc} are the anodic and cathodic peak potentials respectively].

Table 3. Calculated midpoint redox potentials of modified electrodes with $\text{SiO}_2/\text{M}_x\text{O}_y \{ \text{Y}[\text{Fe}(\text{CN})_6] \}^{1-/2-}$; Y=Co, Ni, Cu.

Material	$E_m/\text{V vs SCE}^*$	Ref.
$\text{SiO}_2/\text{SnO}_2[\text{Fe}(\text{CN})_6]^{3-/4-}$	0.22	37
$\text{SiO}_2/\text{SnO}_2\{\text{Co}[\text{Fe}(\text{CN})_6]\}^{1-/2-}$	0.33	52
$\text{SiO}_2/\text{SnO}_2\{\text{Ni}[\text{Fe}(\text{CN})_6]\}^{1-/2-}$	0.46	37
$\text{SiO}_2/\text{SnO}_2\{\text{Cu}[\text{Fe}(\text{CN})_6]\}^{1-/2-}$	0.62	50
$\text{SiO}_2/\text{TiO}_2[\text{Fe}(\text{CN})_6]^{3-/4-}$	0.17	43
$\text{SiO}_2/\text{TiO}_2\{\text{Ni}[\text{Fe}(\text{CN})_6]\}^{1-/2-}$	0.62	51
$\text{SiO}_2/\text{TiO}_2\{\text{Cu}[\text{Fe}(\text{CN})_6]\}^{1-/2-}$	0.76	51
$\text{SiO}_2/\text{ZrO}_2[\text{Fe}(\text{CN})_6]^{3-/4-}$	0.21	44,53
$\text{SiO}_2/\text{ZrO}_2\{\text{Cu}[\text{Fe}(\text{CN})_6]\}^{1-/2-}$	0.69	53

*In 1 mol L^{-1} KNO_3 supporting electrolyte solutions.

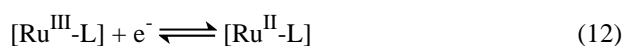
It is shown that E_m depends on the nature of the metal Y in the mixed valence compound, as is observed for bulk phase complexes. Also it is shown that for a given mixed valence complex formed on the surface, E_m depends on the nature of the supporting electrolyte. For instance, in 1 mol L^{-1} NaNO_3 , KNO_3 and NH_4NO_3 , the E_m found (against SCE electrode)³⁷, using the $\text{SiO}_2/\text{SnO}_2\{\text{Ni}[\text{Fe}(\text{CN})_6]\}$ carbon paste electrode, are: 0.35, 0.46 and 0.47 V, respectively. Since the surface mixed valence complex has a zeolitic type structure, such dependence is explained on the basis of the following mechanism proposed for the redox reaction:



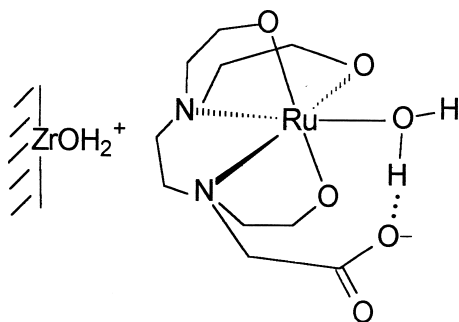
where in the redox process the supporting electrolyte s^+ must diffuse into or move out of the surface structured complex.

The hydrated ionic sizes of the ions are (in nm): $\text{Li}^+ = 0.47$, $\text{Na}^+ = 0.36$, $\text{K}^+ \sim \text{NH}_4^+ = 0.24$ ⁵⁴. Since the channel diameter of the surface complex is 0.31 nm ⁵⁵, ions having nearly the same hydrated radius (NH_4^+ and K^+) have the same midpoint potential and for Na^+ , that presents a larger size, the potential is higher. When using Li^+ as the supporting electrolyte, no redox peak is observed because it can not pass through the cavity of the surface complex. Similar results have been observed with other modified mixed valence complexes adsorbed on $\text{SiO}_2/\text{M}_x\text{O}_y$ ^{37,43-53}.

An interesting example of reactivity of adsorbed species is a property of the adsorbed complex $\text{SiO}_2/\text{ZrO}_2/[\text{Ru}(\text{edta})(\text{H}_2\text{O})]^-$ (Scheme 2)⁵⁶. The adsorbed coordinated H_2O is kinetically labile due to hydrogen bonding and can be easily replaced by a ligand L. If the basicity of ligand L changes, we observe that the midpoint potential of the reaction



depends on the basicity of the ligand L *i.e.*, the more basic the ligand, the more positive will be the midpoint potential (Table 4).



Scheme 2. $[\text{Ru}(\text{edta})(\text{H}_2\text{O})]^-$ adsorbed on $\equiv\text{ZrOH}$; N-N = $\text{NCH}_2\text{CH}_2\text{N}$ and N-O = NCH_2COO^- .

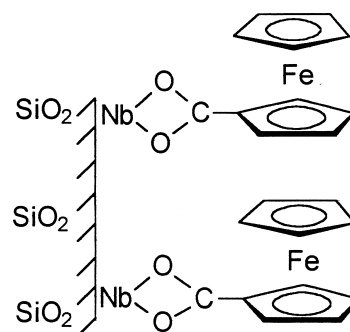
Table 4. Midpoint potentials for $\text{ZrOH}_2^+ / [\text{Ru}(\text{edta})\text{L}]^-$

L	$E_m^*/\text{mV vs SCE}$
H_2O	-290
SCN^-	-200
Pyridine	-180
4-Cyanopyridine	-80
Pyrazine	-50

*solution pH 4.5⁵⁶

In certain cases molecules can be adsorbed onto the substrate surface by a chemical bonding, as is observed for ascorbic acid on $\text{SiO}_2/\text{Nb}_2\text{O}_5$ ⁵⁷. When dipping the solid into a solution containing ascorbic acid, the solid turns yellow immediately, presumably due to the formation of the surface complex. The adsorbed ascorbic acid can efficiently reduce some metal ions at the solid-solution interface. The reduction yield observed for some metal ions is: $\text{Fe}(\text{III}) = 95.4 \pm 2.2\%$,

$\text{Cr}(\text{VI}) = 99.7 \pm 0.2\%$ and $\text{Cu}(\text{II}) = 89.3 \pm 1.6\%$ ⁵⁷. Molecules having a carboxylic acid radical are easily adsorbed on a $\text{SiO}_2/\text{Nb}_2\text{O}_5$ surface due to Nb-OOC- bond formation^{57,58}. Scheme 3 illustrates how ferrocenecarboxylic acid is bound to the $\text{SiO}_2/\text{Nb}_2\text{O}_5$ surface⁵⁹.



Scheme 3. Scheme proposed for binding of ferrocenecarboxylic acid onto the $\text{SiO}_2/\text{Nb}_2\text{O}_5$ surface. (Reproduction from Ref. 59 by permission of Elsevier Science B.V.).

The material $\text{SiO}_2/\text{TiO}_2$ is very efficient as an adsorbent because it is very porous while the bulk phase is normally non-porous. The active sites $\equiv\text{TiOH}$ groups in the former case are distributed over a narrower size pores, and thus, they are more available. When $\text{SiO}_2/\text{TiO}_2$ was immersed in H_2O_2 solution, the coated Ti(IV) oxide exhibited coordination properties. The appearance of an orange color on the solid surface in contact with hydrogen peroxide is a result of the coordination of H_2O_2 with the Lewis acid site⁶⁰. The maximum sorption capacity, $1.2 \text{ molecule nm}^{-2}$, was achieved in solution at pH 3. The adsorbed hydrogen peroxide retained its oxidation capacity for several weeks. After the sorption of the H_2O_2 by $\text{SiO}_2/\text{TiO}_2$, formation of super oxide radicals was observed, presumably resulting from peroxide decomposition.

When the material $\text{SiO}_2/\text{Sb}_2\text{O}_5$ was immersed in an aqueous Fe^{3+} solution, it showed two remarkable changes: an increase of the Sb:Si atomic ratio, due to the enrichment of the amount of Sb(V) content on the matrix surface, and formation of a new phase, FeSbO_4 , as established by the studies of X-ray photoelectron spectroscopy and Mössbauer spectroscopy, respectively⁶¹. With the intention of understanding the mechanism of formation of the FeSbO_4 phase, two different routes for the preparation of the material were studied: (i) $\text{SiO}_2/\text{Sb}_2\text{O}_5$ was immersed in an aqueous solution of Fe^{3+} , followed by thermal treatment at 423 K or (ii) $\text{SiO}_2/\text{Sb}_2\text{O}_5$ was immersed in a solution of $\text{Fe}(\text{CO})_5$ in CCl_4 followed by further hydrolysis and heat treatment at 1073 K^{62,63}. In both cases an excess of Sb(V) was found on the surface, in relation to Fe(III). This fact was interpreted as a result of the migration of Sb(V) from

the internal surface to the external surface when method (i) was used and as being due to migration of Fe(III) in the opposite direction when the material was obtained by method (ii).

6. Applications of $\text{SiO}_2/\text{M}_x\text{O}_y$

6.1 In preconcentration processes and chemical analyses

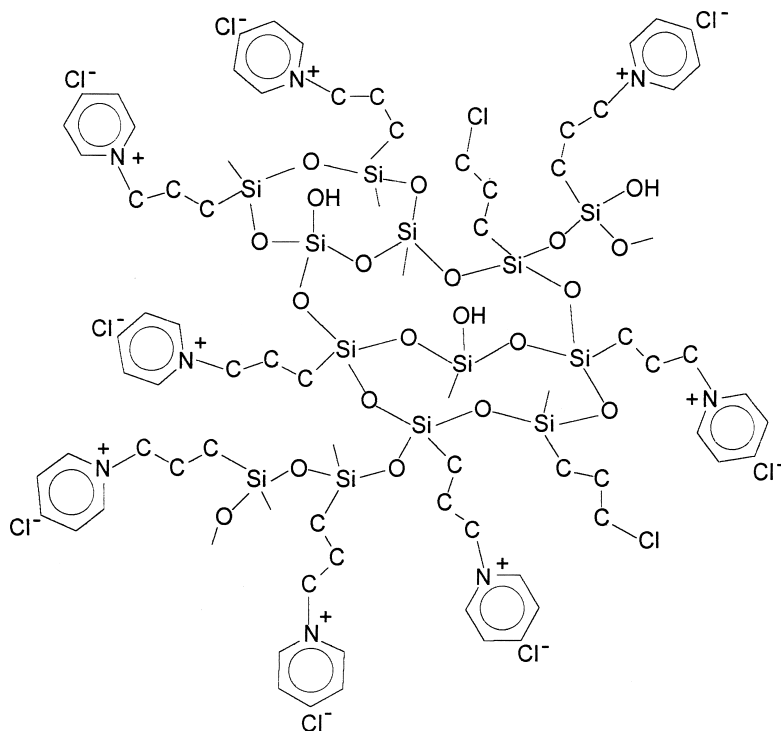
SiO_2/MO_2 (M=Ti, Zr) selectively adsorb $\text{Cr}_2\text{O}_7^{2-}$ from an acid solution^{64,65}:



where MOH stands for hydrated MO_2 grafted on the silica surface. This property has been used to preconcentrate and analyse low concentrations of this ion in water⁶⁶.

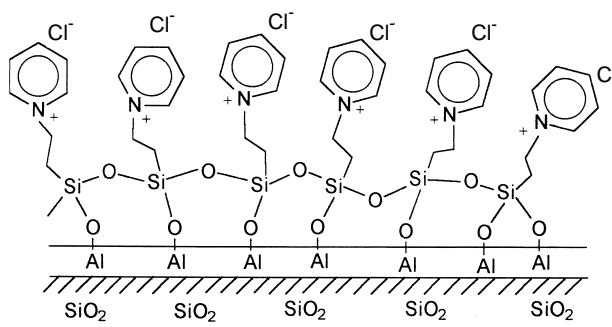
Adsorption properties of metallic ions, such as cadmium, lead and mercury, on $\text{SiO}_2/\text{ZrO}_2$ /phosphate were investigated by using the batch system⁶⁷. A selective adsorption towards heavy metals with increasing affinity order $\text{Cd(II)} < \text{Pb(II)} < \text{Hg(II)}$ was observed. A conjugated use of $\text{SiO}_2/\text{ZrO}_2$ /phosphate and silica modified with n-propylimidazole (SiIm) has been carried out for the separation of heavy-metals, such as cadmium, lead and mercury^{68,69}.

$\text{SiO}_2/\text{Al}_2\text{O}_3$ has been used to adsorb the soluble polyelectrolyte, 3(n-propylpyridinium) chloride silsesquioxane polymer⁷⁰, whose structure is shown in



Scheme 4. Structure of soluble polyelectrolyte, 3(n-propylpyridinium) chloride silsesquioxane polymer.

Scheme 4. The polymer does not immobilize directly onto a SiO_2 surface because it is highly water soluble. However, $\text{SiO}_2/\text{Al}_2\text{O}_3$ has a monolayer of aluminium oxide which can easily react with the free SiOH groups of the polymer, resulting in a layer of the polyelectrolyte strongly adhered to the surface by formation of the Al-O-Si bond, illustrated in Scheme 5. The $\text{SiO}_2/\text{Al}_2\text{O}_3$ with the polyelectrolyte has a very high ion exchange capacity and has been used in adsorption of metal ions from ethanol solutions⁷¹.



Scheme 5. Scheme proposed for a layer of the polyelectrolyte strongly adhered to the $\text{SiO}_2/\text{Al}_2\text{O}_3$ surface by formation of the Al-O-Si bond.

6.2 Support for high-performance liquid chromatography

In high-performance liquid chromatography (HPLC), normally porous SiO_2 covered with organofunctional groups has been used as the stationary phase. However, the use of

this modified substrate has limited chemical stability at pH higher than 7. In addition, silanol groups that were not reacted with organic groups or remained untouched after treatment with end capping reagents, may cause tailing or irreversible adsorption of basic solutes during operation of the column. In recent work, toward overcoming this limitation Collins *et al.* have coated a SiO₂ surface with ZrO₂ or TiO₂ protective layers (monolayer or submonolayer) by a grafting process and, in a further step, treated this material with organofunctional siloxanes such as polymethylsiloxane (PMOS), followed by γ irradiation to promote the cross linking of the organic groups⁷²⁻⁷⁶. A considerable increase in efficiency and excellent stationary phase stability has been observed when using alkaline mobile phases. Figure 2 shows the performance achieved with SiO₂/ZrO₂/PMOS irradiated with γ radiation. Its stability was measured by plotting the relative efficiency against the column volumes of mobile phase using an NH₃/NH₄⁺ buffer pH 10 in MeOH in the proportion 30:70 v/v⁷⁵. Column I refers to SiO₂/PMOS and column II to SiO₂/ZrO₂/PMOS. It is observed that above 1000 column volumes the efficiency for SiO₂/ZrO₂/PMOS is about 95% and for SiO₂/PMOS, is about 75%, of the initially measured efficiencies.

The good results obtained by using SiO₂/MO₂/PMOS (M=Ti, Zr) have been attributed to the reduction of the acidic properties of silica through titanization or zirconization, as well as to PMOS chain cross linking, resulting in stationary phases that show significant promise as a support when high pH mobile phase is required.

6.3 Electrochemical sensors and biosensors

Metal oxides coated on silica gel have been used for immobilization of various electron transfer mediator species. Such modified materials are very attractive because they are the basis for developing various sensors and biosensors. Important characteristics of these materials are

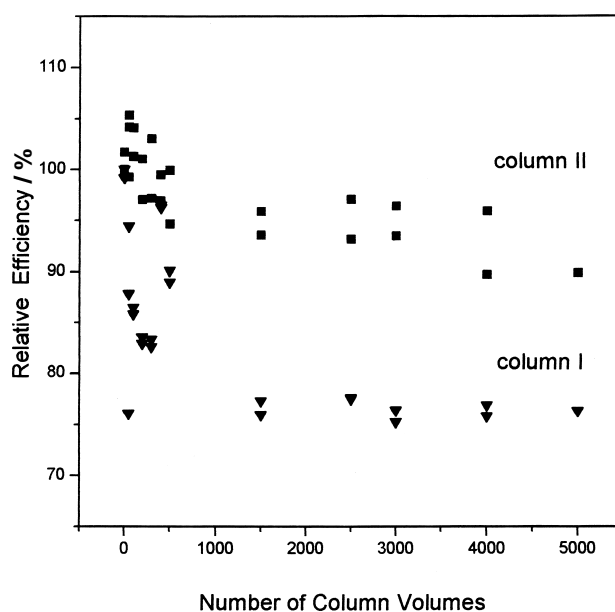


Figure 2. Efficiency vs column volumes using a mobile phase [buffer NH₃/NH₄⁺, pH 10]:MeOH in the proportion 30:70 v/v. Column I refers to SiO₂(PMOS) and column II to SiO₂/ZrO₂(PMOS).

high surface area and porosity, very easy procedures for mediator immobilization, preventing leaching from the electrode into the solution, and the mechanical and chemical resistance conferred by the silica matrix.

The interest in silica-modified electrodes with respect to their applications in electroanalysis was recently reviewed by Walcarus⁷⁷. Table 5 presents a short summary of the use of SiO₂/M_xO_y-containing electrodes for the development of electrochemical sensors and biosensors.

The following overview describes the main uses found for these materials up to now.

6.3.1 Ascorbic acid sensor

The hexacyanoferrate ion adsorbed on SiO₂/ZrO₂ has been used to quantitatively determine vitamin C in natural

Table 5. Applications of modified carbon paste electrodes with modified silica in chemical analysis.

Analyte	Modifier [a]	Detection medium (pH and concentration) [b]	Method (E _{appl} in mV vs SCE)	Concentration range	Ref.
Hydrazine	ST-NiTsPc	Acetate (pH 7, 0.5 mol L ⁻¹)	Amperometry (480)	1x10 ⁻⁴ – 6x10 ⁻⁴ mol L ⁻¹	80
Cysteine	ST-NiTsPc	Acetate (pH 2, 0.5 mol L ⁻¹)	Amperometry (500)	1x10 ⁻³ – 7x10 ⁻³ mol L ⁻¹	79
Hydrazine	ST-FeTsPc	KCl (pH 6, 1 mol L ⁻¹)	Cyclic Voltammetry		78
NADH	STPM	Phosphate buffer (pH 7.4)	Amperometry (0)	1x10 ⁻⁵ – 5x10 ⁻⁵ mol L ⁻¹	45
O ₂	SNb-CoHMP	KCl (pH 6, 1 mol L ⁻¹)	Cyclic Voltammetry	8.4x10 ⁻⁵ – 3.9x10 ⁻⁴ mol L ⁻¹	58
O ₂	SNb-CoPP	KCl (pH 6, 1 mol L ⁻¹)	Cyclic Voltammetry	5x10 ⁻⁵ – 3.4x10 ⁻⁴ mol L ⁻¹	58
Glucose	ST-FC-GOD	PIPES (pH 6.8, 0.1 mol L ⁻¹)	Amperometry (?)	1x10 ⁻⁴ – 8x10 ⁻⁴ mol L ⁻¹	83
Fructose	STPM-FDH	McIlvaine (pH 4.5)	Amperometry (20)	1x10 ⁻⁴ – 7x10 ⁻⁴ mol L ⁻¹	46
Salicylate	STPM-SH	Phosphate buffer (pH 7.4)	Amperometry (200)	1x10 ⁻⁵ – 6x10 ⁻⁵ mol L ⁻¹	47
Phenol	ST-HRP	Phosphate buffer (pH 7)	Amperometry (0)	1x10 ⁻⁵ – 5x10 ⁻⁵ mol L ⁻¹	84

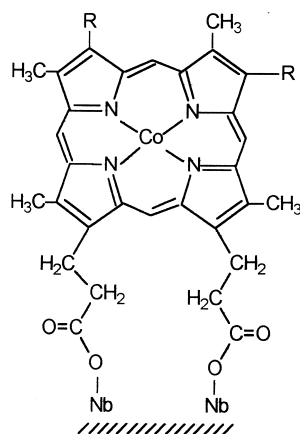
[a] Abbreviations: ST = SiO₂/TiO₂; STPM = SiO₂/TiO₂/phosphate/Meldola's Blue; SNb = SiO₂/Nb₂O₅; CoHMP = cobalt (II) hematoporphyrin IX; CoPP = cobalt (II) protoporphyrin IX; NiTsPc = nickel tetrasulfophthalocyanine; FeTsPc = iron tetrasulfophthalocyanine; HRP = horseradish peroxidase; FDH = D-fructose 5-dehydrogenase; GOD = glucose oxidase; SH = salicylate hydroxylase; [b] Abbreviations: PIPES = 1,4-piperazinediethanesulfonic acid.

and processed juices, as well as in tablets⁴⁴. The hexacyano-ferrate anion can mediate the catalytic oxidation of ascorbic acid at lower potential and thus avoid interference from other species normally present in real samples.

6.3.2 Dissolved oxygen sensor

The material $\text{SiO}_2/\text{ZrO}_2/[\text{Ru}(\text{edta})(\text{H}_2\text{O})]^-$ was used to fabricate an amperometric sensor for determination of dioxygen in natural water⁵⁶. On this electrode surface dissolved O_2 is reduced at -300 mV vs SCE, against -500 mV on a bare electrode surface. The electrode is very selective and the use of a semi permeable membrane, as used in the Clark electrode, is not necessary in the present case. The lower limit of detectable dissolved oxygen is about 0.5 mg L^{-1} .

Cobalt (II) hematoporphyrin IX or cobalt (II) protoporphyrin IX are adsorbed on $\text{SiO}_2/\text{Nb}_2\text{O}_5$ surface by Nb-OOC- chemical bond formation⁵⁸ (Scheme 6). In the presence of dissolved O_2 , a cathodic peak at -0.18 V (vs SCE) is observed. Between pH 4 and 7, the electrode response is not affected, keeping the cathodic potential constant.



R: $-\text{CH}(\text{OH})-\text{CH}_3$, Hematoporphyrin IX; $-\text{C}(\text{H})=\text{CH}_2$, Protoporphyrin IX

Scheme 6. Scheme of the Co(II) metallated porphyrins immobilized on $\text{SiO}_2/\text{Nb}_2\text{O}_5$.

6.3.3 Hydrazine and cysteine sensor

The catalytic properties of metallophthalocyanines immobilized on $\text{SiO}_2/\text{TiO}_2$ have been explored as sensors for the indicated chemical species⁷⁸⁻⁸⁰. Iron tetra-sulfophthalocyanine immobilized on $\text{SiO}_2/\text{TiO}_2$ shows great stability in acid⁷⁸. In a similar way, nickel tetra-sulfophthalocyanine immobilized on $\text{SiO}_2/\text{TiO}_2$ was used for development of an electrochemical sensor for hydrazine⁷⁹.

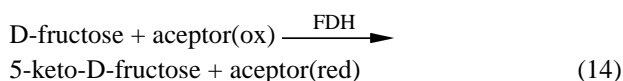
6.3.4 NADH sensor

Meldola's blue (MB) immobilized on a $\text{SiO}_2/\text{TiO}_2/\text{Phosphate carbon paste electrode}$ ⁴⁵ is an effective electron mediator for NADH.

Methylene blue was immobilized on a $\text{SiO}_2/\text{Nb}_2\text{O}_5$ surface and a carbon paste electrode of this material was also tested to oxidize NADH⁸¹. An important characteristic of the electrode is that the redox potential was not affected between pH 4 and 7.

6.3.5 Fructose biosensor

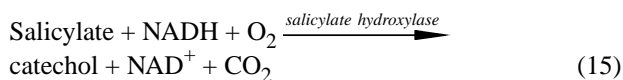
A carbon paste electrode made with $\text{SiO}_2/\text{TiO}_2/\text{Phosphate/MB}$ was used as a biosensor for fructose⁴⁶ and salicylate⁴⁷. In both cases, the presence of the mediator allowed the application of a low overpotential for the detection of the analytes. The electrode was prepared by incorporating fructose 5-dehydrogenase (FDH). The enzyme FDH catalyses the oxidation of D-fructose to 5-keto-D-fructose⁸²:



This biosensor was used to determine fructose in sweets and fruit jellies.

6.3.6 Salicylate biosensor

In the case of the biosensor for salicylate⁴⁷, the reaction catalysed by the enzyme salicylate hydroxylase can be represented by the equation:



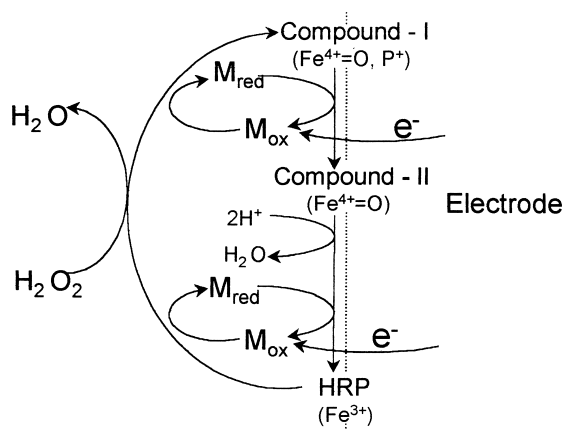
The consumption of NADH or O_2 or the formation of catechol or CO_2 can be measured and are proportional to the salicylate concentration. This biosensor detects the catechol produced in the enzymatic reaction through its electrooxidation on the mediator.

6.3.7 Glucose biosensor

The immobilization of ferrocene carboxylic acid and the enzyme glucose oxidase on the surface of $\text{SiO}_2/\text{TiO}_2$ was reported⁸³. The electrode is used to determine glucose in blood serum⁸³. The mechanism of the electron transfer was proposed as being electron tunnelling by the flavin of the enzyme to the mediator, and the high current level was assigned to the high surface area of the silica matrix. The immobilized material presented excellent stability, maintaining the same activity for at least six months.

6.3.8 Phenol biosensor

Recently, Kubota *et al.*⁸⁴ immobilized horseradish peroxidase on SiO₂/TiO₂ and used this for biosensor development. The direct electron transfer of hydrogen peroxide reduction by HRP was blocked by immobilizing the enzyme on silica-titanium. In this case, the sensitivity of the biosensor improved significantly, obtaining a device with better characteristics with respect to sensitivity and operational range. The mechanism of electrode response mediated for phenol can be visualized in Scheme 7.



Scheme 7. Mechanism of mediated electron transfer at SiO₂/TiO₂/HRP-modified carbon paste electrode. M_{ox} and M_{red} are the oxidized and reduced forms of the mediator, respectively. (Reproduction from Ref. 84 by permission of Elsevier Science B.V.).

The stability of this electrode configuration was lower, compared to that obtained for the peroxidase immobilized directly onto graphite, probably due to its environment. The influence of different additives, like bovine serum albumin (BSA), polyethylenimine (PEI) and DNA, on the sensitivity and operational stability of a phenol biosensor based on peroxidase immobilized on silica-titanium and mixed in carbon was studied⁸⁵. The high sensitivity of the biosensor and the stability obtained by DNA incorporation permitted phenol determination in real samples of industrial effluents and the waters of polluted rivers. The results showed that the biosensor is more sensitive for phenol determination in the different types of samples, in comparison to the spectrometric method.

6.3.9 Affinity biosensor

SiO₂/TiO₂ was also used as a base for the immobilization of a single-stranded oligonucleotide⁸⁶. Such immobilization proceeds through the reaction of the titanium oxide monolayer (on the silica surface) with the phosphate backbone of the oligonucleotide probe, leaving the nucleobases readily accessible for the hybridisation event.

The use of SiO₂/TiO₂ results in a homogeneous dispersion of the nucleic acid probe within the interior of the carbon paste composite. The hybridisation response obtained with this format of a DNA biosensor was reproducible.

7. Conclusions

Metal oxides highly and uniformly dispersed as thin monolayer surfaces on a silica gel surface constitute a class of new materials which provide a relatively inert support possessing high chemical and thermal stabilities. Despite its insulating nature, they can be successfully be used in fabrication of electrochemical devices such as electrochemical sensors. The high sensitivity achieved by using such kinds of materials is mainly due to the porous character of the SiO₂ matrix used to prepare most of the materials described in this work. A very important aspect is that the matrix is rigid and does not swell when immersed in a liquid phase. From a thermodynamic point of view, such behaviour is sometimes desirable, because interface phenomena are more predictable and thus easier to study and more clearly understandable.

Recent reports have shown the potential use of these materials, especially in the construction of a class of highly sensitive electrochemical sensors⁵⁶. Other possibilities are: in enzyme immobilizations, for use in water desalination processes, for using these materials as adsorbents of chemical species in non-aqueous solvents, for specific chemical reactions of the immobilized species and as very promising materials for use in HPLC.

Acknowledgments

The authors thank FAPESP for financial support and Professor Carol Collins for the English revision of the manuscript.

References

1. Ellestad, O. H.; Blindheim, U. *J. Mol. Catal.* **1985**, *33*, 275.
2. Ko, E. I.; Bafrafi, R.; Nuhfer, N. T.; Wagner, N. J. *J. Catal.*, **1985**, *95*, 260.
3. Nishimura, M.; Asakura, K.; Iwasawa, Y. *J. Chem. Soc., Chem. Commun.* **1986**, 1660.
4. Asakura, K.; Iwasawa, Y. *Chem. Lett.*, **1986**, 859.
5. Nishimura, M.; Asakura, K.; Iwasawa, Y. *Chem. Lett.*, **1986**, 1457.
6. Bond, G. C.; Flamerz, S.; Shukri, S. *Faraday Discuss. Chem. Soc.* **1989**, *87*, 65.
7. Getty, E. E.; Drago, R. S. *Inorg. Chem.* **1990**, *29*, 1186.

8. Shirai, M.; Ichikuni, N.; Iwasawa, Y. *Catal. Today* **1990**, *8*, 57.
9. Ichikuni, N.; Asakura, K.; Iwasawa, Y. *J. Chem. Soc. Chem. Commun.*, **1991**, 112.
10. Asakura, K.; Iwasawa, Y. *J. Phys. Chem.* **1991**, *95*, 1711.
11. Shirai, M.; Asakura, K.; Iwasawa, Y. *J. Phys. Chem.* **1991**, *95*, 9999.
12. Kubota, L. T.; Gushikem, Y.; de Castro, S. C.; Moreira, J. C. *Colloids Surf.* **1991**, *57*, 11.
13. Drago, R. S.; Petrosius, S. C.; Chronister, C. W. *Inorg. Chem.* **1994**, *33*, 367.
14. Inoue, Y.; Yamazaki, H.; Kimura, Y. *Bull. Chem. Soc. Jpn* **1985**, *116*, 281.
15. Slotfeldt-Ellingsen, D.; Dahl, I.M.; Ellestad, O.H. *J. Mol. Catal.* **1980**, *9*, 423.
16. Riis, T.; Dahl, I. M.; Ellestad, O. H. *J. Mol. Catal.* **1983**, *18*, 203.
17. Baltés, M.; Collart, O.; Van Der Voort, P.; Vansant, E. F. *Langmuir* **1999**, *15*, 5841.
18. Wachs, I. E.; Deo, G.; Vuurman, M. A.; Hu, H.; Kim, D. S.; Jehng, J. *J. Mol. Catal.* **1993**, *82*, 443.
19. Collart, O.; Van Der Voort, P.; Vansant, E. F.; Gustin, E.; Bowen, A.; Schoemaker, D.; Rao, R. R.; Weckhuysen, B. M.; Schoonheydt, R. A. *Phys. Chem. Chem. Phys.* **1999**, *1*, 4099.
20. Meijers, A. C. Q. M.; de Jong, A. M.; Van Gruijthuisen, L. M. P.; Niemantsverdriet, J. W. *Appl. Catal.* **1991**, *70*, 53.
21. Damyanova, S.; Grange, P.; Delmon, B. *J. Catal.* **1997**, *168*, 421.
22. Gao, X.; Fierro, J. L. G.; Wachs, I. E. *Langmuir* **1999**, *15*, 3169.
23. Sohn, J. R.; Jang, H. J. *J. Mol. Catal.* **1991**, *64*, 349.
24. Drago, R. S.; Getty, E. E. *J. Am. Chem. Soc.* **1988**, *110*, 3311.
25. Fisher, I. A.; Woo, H. C.; Bell, A. T. *Catal. Lett.* **1997**, *44*, 11.
26. Naito, S.; Tanimoto, M. *J. Catal.* **1995**, *154*, 306.
27. Denofre, S.; Gushikem, Y.; de Castro, S. C.; Kawano, Y. *J. Chem. Soc. Faraday Trans.* **1993**, *89*, 1057.
28. Weissman, J. G.; Ko, E. I.; Wynblatt, P. *J. Catal.* **1987**, *108*, 383.
29. Birchall, T.; Connor, J. A.; Hillier, I. H. *J. Chem. Soc. Dalton Trans. 1* **1975**, *71*, 2003.
30. Garbassi, F. *Surf. Interface Anal.* **1980**, *2*, 165.
31. Fontaine, R.; Caillat, R.; Feve, L.; Guittet, M. J. *J. Electron Spectrosc.* **1977**, *10*, 349.
32. Wagner, C. D. (Ed.), *Handbook of X-Ray Photoelectron Spectroscopy*, Perkin-Elmer, Eden Prairie, MN, 1979.
33. Ikeya, T.; Senna, M. *J. Non-Cryst. Solid* **1988**, *105*, 243.
34. Prado, L. L. L.; Nascente, P. A. P.; de Castro, S. C.; Gushikem, Y. *J. Mater. Sci.* **2000**, *35*, 449.
35. Peixoto, C. R. M.; Kubota, L. T.; Gushikem, Y. *Anal. Proc.* **1995**, *32*, 503.
36. Benvenuti, E. V.; Gushikem, Y.; Davanzo, C. U.; de Castro, S. C.; Torriani, I. L. *J. Chem. Soc. Faraday Trans.* **1992**, *88*, 3193.
37. Zaldivar, G. A. P.; Gushikem, Y. *J. Electroanal. Chem.* **1992**, *337*, 165.
38. Benvenuti, E. V.; Gushikem, Y.; Davanzo, C. U. *Appl. Spectrosc.* **1992**, *46*, 1474.
39. Goodenough, J. B.; Manoharan, R.; Paranthaman, M. *J. Am. Chem. Soc.* **1990**, *112*, 2076.
40. Parks, G. A. *Chem. Reviews* **1965**, *65*, 177.
41. Kita, H.; Henmi, N.; Shimazu, K.; Hattori, H.; Tanabe, K. *J. Chem. Soc. Faraday Trans.* **1981**, *77*, 2451.
42. Shriver, D. F. *J. Am. Chem. Soc.* **1963**, *85*, 1405.
43. Kubota, L. T.; Gushikem, Y. *Electrochim. Acta* **1992**, *37*, 2477.
44. Andreotti, E. I. S.; Gushikem, Y.; Kubota, L. T. *J. Braz. Chem. Soc.* **1992**, *3*, 21.
45. Kubota, L. T.; Gouvêa, F.; Andrade, A. N.; Milagres, B. G.; Oliveira Neto, G. *Electrochim. Acta* **1996**, *41*, 1465.
46. Garcia, C. A. B.; Oliveira Neto, G.; Kubota, L. T.; Grandin, L. A. *J. Electroanal. Chem.* **1996**, *418*, 147.
47. Kubota, L. T.; Milagres, B. G.; Gouvea, F.; Oliveira Neto, G. *Anal. Lett.* **1996**, *29*, 893.
48. Rocha, R. F.; Rosatto, S. S.; Bruns, R. E.; Kubota, L. T. *J. Electroanal. Chem.* **1997**, *433*, 73.
49. Peixoto, C. R. M.; Kubota, L. T.; Gushikem, Y. *J. Braz. Chem. Soc.* **1995**, *6*, 83.
50. Zaldivar, G. A. P.; Gushikem, Y.; Kubota, L. T. *J. Electroanal. Chem.* **1991**, *318*, 247.
51. Kubota, L. T.; Gushikem, Y. *J. Electroanal. Chem.* **1993**, *362*, 219.
52. Zaldivar, G. A. P.; Gushikem, Y.; Benvenuti, E. V.; de Castro, S. C.; Vasquez, A. *Electrochim. Acta* **1994**, *39*, 33.
53. da Cunha, L. J.V.; Andreotti, E. I.S.; Gushikem, Y. *J. Braz. Chem. Soc.* **1995**, *6*, 271.
54. Moelwyn-Hughes, E. A. *Physical Chemistry*, Pergamon Press, London, 1961, p 587.
55. Seifer, G. S. B. *Russ. J. Inorg. Chem.*, **1962**, *7*, 621.
56. Gushikem, Y.; Peixoto, C. R. M.; Rodrigues Filho, U. P.; Kubota, L. T.; Stadler, E. *J. Colloid Interface Sci.* **1996**, *184*, 236.
57. Denofre, S.; Gushikem, Y.; Davanzo, C. U. *Eur. J. Solid State Inorg. Chem.* **1991**, *28*, 1295.
58. Pessôa, C. A.; Gushikem, Y. *J. Electroanal. Chem.* **1999**, *477*, 158.
59. Pessôa, C. A.; Gushikem, Y.; Kubota, L. T. *Electrochim. Acta* **2001**, *46*, 2499.

60. Kubota, L. T.; Gushikem, Y.; Mansanares, A. M.; Vargas, H. *J. Colloid Interface Sci.* **1995**, *173*, 372.
61. Benvenutti, E. V.; Gushikem, Y.; Vasquez, A.; de Castro S. C.; Zaldivar, G. A. P. *J. Chem. Soc., Chem. Commun.* **1991**, 1325.
62. Davanzo, C. U.; Gushikem, Y.; de Castro, S. C.; Benvenutti, E. V.; Vasquez, A. *J. Chem. Soc., Faraday Trans.* **1996**, *92*, 1569.
63. Benvenutti, E. V.; Gushikem, Y. *J. Braz. Chem. Soc.* **1998**, *9*, 469.
64. Kubota, L. T.; Gushikem, Y.; Moreira, J. C. *Analyst* **1991**, *116*, 281.
65. Gushikem, Y.; Peixoto, C. R. M.; Kubota, L. T. In *New Developments in Ion Exchange. Materials, Fundamentals and Applications*, Proceedings of the International Conference on Ion Exchange, ICIE'91, Tokyo, Jpn, 1991, 607.
66. Peixoto, C. R. M.; Gushikem Y.; Baccan, N. *Analyst* **1992**, *117*, 1029.
67. Nagata, N.; Kubota, L. T.; Bueno M. I. M. S.; Peralta-Zamora, P. G. *J. Colloid Interface Sci.* **1998**, *200*, 121.
68. Nagata, N.; Peralta-Zamora, P. G.; Kubota, L. T.; Bueno, M. I. M. S. *Anal. Sci.* **1999**, *15*, 761.
69. Nagata, N.; Peralta-Zamora, P. G.; Kubota L. T.; Bueno, M. I. S. *Anal. Lett.* **2000**, *33*, 2005.
70. Gushikem, Y.; Alfaya R. V. S.; Alfaya, A. A. S. Brazilian Patent, BR9803053-A **1998**.
71. Fujiwara, S. T.; Gushikem Y.; Alfaya, R. V. S. *Colloids Surf., A* **2001**, *178*, 135.
72. Silva R. B.; Collins, C. H. *J. Chromatogr., A* **1999**, *845*, 417.
73. Melo L. F. C.; Jardim, I. C. S. F. *J. Chromatogr., A* **1999**, *845*, 423.
74. Silva, R. B.; Collins K. E.; Collins, C. H. *J. Chromatogr., A* **2000**, *869*, 137.
75. Melo, L. F. C.; Collins, C. H.; Collins K. E.; Jardim, I. C. S. F. *J. Chromatogr., A* **2000**, *869*, 129.
76. Silva, R. B.; Gushikem Y.; Collins, C. H. *J. Sep. Sci.* **2001**, *24*, 1.
77. Walcarius, A. *Electroanalysis* **1998**, *10*, 1217.
78. Kubota, L. T.; Gushikem, Y.; Perez, J.; Tanaka, A. A. *Langmuir* **1995**, *11*, 1009.
79. Perez, E. F.; Kubota, L. T.; Tanaka, A. A.; Oliveira Neto, G. *Electrochim. Acta* **1998**, *43*, 1665.
80. Perez, E. F.; Oliveira Neto, G.; Tanaka, A. A.; Kubota, L. T. *Electroanalysis* **1998**, *10*, 111.
81. Schiavo, D. A.; Perez, E. F.; Kubota, L. T. *Quim. Nova* **2000**, *23*, 832.
82. Yamada, Y.; Aida K.; Uemura, I. *Agric. Biol. Chem.* **1966**, *30*, 95.
83. Milagres, B. G.; Kubota, L. T.; Oliveira Neto, G. *Electroanalysis* **1996**, *8*, 489.
84. Rosatto, S. S.; Kubota, L. T.; Oliveira Neto, G. *Anal. Chim. Acta* **1999**, *390*, 65.
85. Rosatto, S. S.; Kubota, L. T.; Oliveira Neto, G. *Electroanalysis* **2001**, *13*, 445.
86. Wang, J.; Fernandes, J. R.; Kubota, L. T. *Anal. Chem.* **1998**, *70*, 3699.

Received: May 4, 2001

Published on the web: September 13, 2001

FAPESP helped in meeting the publication costs of this article.